Vol. 46, No. 4 (2024) 596-610, DOI: 10.24874/ti.1672.04.24.07

Tribology in Industry

www.tribology.rs

RESEARCH

Fabrication and Characterization of Physical, Mechanical, and Wear Characteristics of AA7075/SiC Composites by Floating Die

Ameen Al Njjar[a,b,*], Kamar Mazloum[a,b], Amit Sata[a]

[a]*Department of Mechanical Engineering, Faculty of Technology, Marwadi University, Rajkot 360003, India,*
[b]*Department of Mechanical Design Engineering, Faculty of Mechanical and Electrical Engineering, Damascus University, Damascus, Syria.*

Keywords:

Floating die
Powder metallurgy (PM)
Wear Behavior
Physical and mechanical properties
ANOVA
Taguchi
Response surface method

* Corresponding author:

Ameen Al Njjar
E-mail: ameen.alnjjar111669@marwadiuniversity.ac.in

Received: 29 April 2024
Revised: 2 June 2024
Accepted: 28 July 2024

A B S T R A C T

The study investigates AA7075-based matrix composites, renowned for their strength and wear resistance, with a focus on aerospace and automotive applications. Using powder metallurgy with floating die-pressing, composites with varying SiC weight proportions (0%, 5%, 10%, 15%) were synthesized and thoroughly analyzed for physical, mechanical, and microstructural properties. Through L9 orthogonal array experiments, the effects of SiC weight percentage, sliding distance, load, and sliding speed on tribological behavior were studied, employing Taguchi's analysis and ANOVA to understand and quantify these effects. Regression equations, contour plots, and surface plots generated using the response surface method helped visualize the relationships between these factors. The composite containing 5% SiC demonstrated superior properties, including a substantial increase in compressive strength (20.1%), weight reduction (13.7%), and a significant decrease in wear loss (83.28%), making it highly promising for aerospace, defense, and automotive sectors. Additionally, uniform failure models were observed in compression tests of composites fabricated using the floating die method. ANOVA analysis revealed that wear loss was primarily influenced by sliding distance (77.13%), followed by SiC weight percentage (11.77%), sliding speed (9.68%), and load (1.42%). The coefficient of friction (COF) was affected by SiC weight percentage (47.54%), followed by sliding distance (22.72%), load (19.14%), and sliding speed (10.59%).

1. INTRODUCTION

Aluminum alloys are becoming more and more popular for structural applications, especially in the aerospace and automotive industries. Their exceptional properties, which include high specific power, low density, superior heat conductivity, and an excellent strength-to-weight ratio, are responsible for this trend. When combined, these qualities offer significant economic benefits [1]. The

enhanced material properties observed with varying SiC weight proportions, such as improved strength, wear resistance, and weight reduction, are crucial for high-performance applications in these fields. For instance, in aerospace and defense, materials with superior strength-to-weight ratios are essential for structural components, where reducing the weight of materials used in vehicles will lower fuel consumption. In the automotive industry, improved wear resistance, mechanical properties, and weight reduction can lead to longer-lasting, more reliable components, while also reducing fuel consumption and CO2 emissions. Reports indicate that reducing a car's weight by 10% can increase fuel economy by 8–10% and reduce CO2 emissions by 12.5 g/km for every 100 kg weight reduction [2-4]. Aluminum-based metal matrix composites have become increasingly popular due to their low weight, high modulus, strength, stiffness, and resistance to wear and corrosion. Most composites have better mechanical characteristics than traditional metals and alloys [5,6]. Adding different ceramic particles to the Aluminium matrix changes its characteristics, which are then used in a variety of industrial sectors [7].

Many scholars are concentrating their efforts on composites incorporating ZrO_2, Al_2O_3, graphene, TiC, B_4C, and SiC due to their improved tribological and mechanical properties [5–13]. Choosing the right fabrication technique is crucial when it comes to metal matrix composites. A wide range of methods, including powder metallurgy, centrifugal casting, chemical vapor deposition, thermal spraying, and hot pressing, can be used to create these composites [17–19].

Among all the approaches that are accessible, powder metallurgy is one of the easiest and most economical. This is because it can control density and composition to create composites that almost perfectly resemble the required shape [20–23]. In powder metallurgy, the compaction process is crucial because it determines how the final product's mechanical and physical qualities are distributed. For this, a variety of die types can be used, such as floating die (FD), double action (DA), and single action (SA) die. In a SA die, the powder is compressed by the upper punch while the die stays stationary. On the other hand, with a die for DA, the powder in the stationary die is compressed by both the upper and lower punches. Nonetheless, in contrast to the intricate mechanism of the DA die, the FD die is frequently regarded as the most effective and economical die type. Furthermore, with the FD die, the lower punch remains fixed while the upper punch moves together with the die to exert pressure on the powder [24].

The microstructure of composites, the type and amount of reinforcement utilized, and the degree of interfacial bonding between the reinforcement and matrix all have a major impact on their mechanical properties [25]. Numerous parameters, including the disc's material, lubricant type, load, sliding distance, and reinforcing weight percentage, have a significant impact on the tribological characteristics of the composites [26,27].

Drawing from the findings of an exhaustive review of the literature, many researchers have delved into diverse classifications of Aluminum. However, previous investigations primarily utilized a single-action die in composite manufacturing, resulting in uneven dispersion of physical and mechanical properties throughout the composite samples, as opposed to the more effective distribution that can be achieved through a floating die [24].

This investigation focused on fabricating AA7075 metal matrix composites by integrating varying weight percentages (0%, 5%, 10%, and 15%) of silicon carbide (SiC) through an innovative floating die pressing method within the domain of powder metallurgy. A comprehensive analysis was conducted on the microstructure, physical attributes, tribological and mechanical characteristics. Statistical methodologies including ANOVA, Taguchi analysis, and response surface method were utilized to assess the influence of tribological variables on both coefficient of friction (COF) and wear loss. The impact of tribological factors on COF and wear loss was examined using Taguchi analysis, and the percentage of each factor that contributed to the final properties was ascertained using ANOVA. Regression equations were also derived using the response surface method. Overall, the results showed that AA7075-SiC composites made with the floating die technique had good qualities, which made them appropriate for uses that require materials with high strength, low weight, and wear resistance, particularly in the fields of aerospace, defense, and automotive engineering.

2. EXPERIMENTAL PROCEDURE

The investigation utilized Aluminium Alloy AA7075 powder as the matrix material, characterized by an average particle size (APS) of 50 microns and a density of 2.81 g/cc. Silicon carbide (SiC) powder, with an APS of 10 microns and a density of 3.21 g/cc, served as the reinforcing material. Table 1 illustrates the chemical composition of AA7075.
Two types of dies were employed for powder compaction: floating dies (FD) and single-action dies (SA). Table 2 outlines the composite formulations based on AA7075 with varying SiC percentages (0%, 5%, 10%, and 15%) and die types used for compaction.

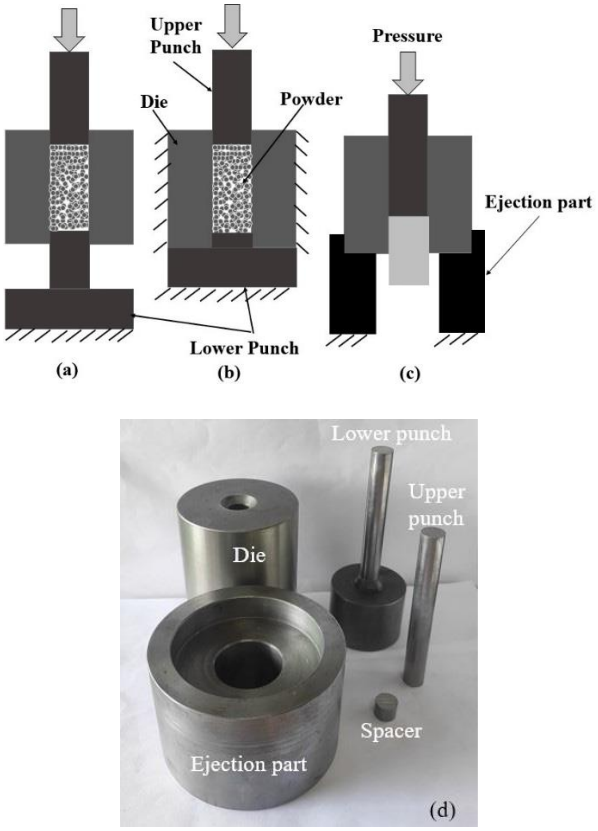

Fig. 1. Drawings diagram of (a) FD method, (b) SA method, (c) Ejection procedure, (d) Die parts.

Fig. 1 showcases illustrations of the floating die (FD) (Fig. 1a) and single-action die (SA) (Fig. 1b), the procedure for ejecting the compacted sample (Fig. 1c), and the components of the die (Fig. 1d). In both compaction techniques, the lower punch remains fixed. However, in the floating die (Fig. 1a), the friction between the powder and die wall, along with the freedom of movement along the die axis, allows the die to move by applying pressure on the top punch. Samples measuring 25mm in height were prepared using a die featuring a cavity diameter of 13mm in both the SA and FD methods. Powder blending was conducted using a ball mill at 100 rpm for one hour with a ball-to-powder ratio of 10:1 [28].

The mixed powder was compacted under a pressure of 300 MPa. Following this, the compacted samples underwent sintering in a controlled and enclosed atmospheric environment in a muffle furnace at 620°C for 120 minutes [29]. The sintered samples obtained are illustrated in Fig. 2.

Table 1. Composition of AA7075.

Al	Cr	Zn	Fe	Si	Ni	Ga	Cu
91.33%	0.03 %	6.94 %	0.32 %	0.5 %	0.01 %	0.03 %	0.84 %

Table 2. The composites with different proportions of SiC and different die types.

Composites. ID	Die Type	Wt.% SiC	Wt.% AA7075
A-SA	Single Action Die (SA)	0	100
A-FD	Floating Die (FD)	0	100
A5S-FD	Floating Die (FD)	5	95
A10S-FD	Floating Die (FD)	10	90
A15S-FD	Floating Die (FD)	15	85

Fig. 2. The sintered composite samples.

The Archimedes principle was utilized to ascertain the density and porosity of the produced composites. Additionally, the rule of mixture was employed to calculate theoretical densities based on the percentage of reinforcement weight, as outlined in Equation (1) [30]

$$\rho_c = \rho_r * V_r + \rho_m * V_m \quad (1)$$

Where,
ρ_r: Theoretical density of reinforced material, V_r: Percentage of the reinforced material, ρ_c: Theoretical density of the composite, ρ_m: Theoretical density of matrix material, V_m: Percentage of the matrix material.

Porosity stands as a critical physical attribute significantly affecting the tribological and mechanical characteristics of the composite. The predominant factors influencing composite porosity include mechanical alloying, sintering temperature, and compaction pressure. Equation (2) enables the calculation of the observed density of the sintered composites [31].

$$\rho = (\frac{W}{W-W_1})^* \rho_1 \quad (2)$$

Where,
W: Sintered composite weight in the air[g], W_1: Sintered composite weight in water[g], ρ: Measured density of the sintered composite [g/cm^3], ρ_1: Water density [g/cm^3].

The porosity percentages(P%) of the prepared composites were determined using Equation (3) [32].

$$P\% = \frac{Theoritical\ density - Measured\ density}{Theoritical\ density} * 100 \quad (3)$$

Additionally, silicon carbide paper grading from 400 to 2500 was used to prepare the samples for microstructure investigation. After that, 1µm diamond paste was used for polishing. Subsequently, they were etched with Keller reagent (190 ml of distilled water,3 ml of HCl +2 ml of HF, and 5 ml of HNO_3) [33]. An optical microscope (Metzer-M) was then used to examine the specimens' microstructure, allowing for observation and analysis.

At room temperature, a universal testing machine was used to perform a compression test. Rockwell hardness test was performed using a digital hardness test device (Model: SE-RSNE, manufactured by Samarth Engineering, India), following the ASTM E18-15 standard. This test utilizes a 100 Kgs load with a 1/16th inch steel indenter [28]. The hardness of each sample was determined by averaging seven measurements.

In accordance with ASTM G99-05 specifications, dry sliding wear examinations were carried out on cylindrical pins using pin-on-disc equipment [34]. The sintered samples were machined to dimensions of 25 mm in length and 10 mm in diameter using a lathe machine. To ensure uniform surface roughness before the wear test, all sliding surfaces of the pins were prepared with emery sheets grade of 400 to 1000.

Additionally, ANOVA, the response surface method, and the L9 orthogonal array were employed to optimize the wear characteristics of the AA7075/SiC composites. Wear studies were conducted by varying the weight percent of SiC, load, sliding distance, and sliding speed. Table 3 presents the different factors and their corresponding levels utilized in this study. Additionally, Table 4 illustrates the nine distinct tests with varying factors and levels using the L9 orthogonal array.

Table 3. The tribological parameters and levels.

Icon	Parameters	Level I	Level II	Level III	Units
W	Wt.% SiC	0	5	10	%
SD	Sliding Distance	500	1000	1500	(m)
L	Load	5	10	15	(N)
SS	Sliding Speed	1	1.5	2	(m/s)

Table 4. Wear tests as L9 orthogonal array.

Exp. No	W (%)	L (N)	SD (m)	SS (m/s)
1	0	5	500	1
2	0	10	1000	1.5
3	0	15	1500	2
4	5	5	1000	2
5	5	10	1500	1
6	5	15	500	1.5
7	10	5	1500	1.5
8	10	10	500	2
9	10	15	1000	1

Table 5. The required time and disc speed.

Exp. No	Required time (s)	Disc Speed (R.P.M)
1	500	238
2	667	358
3	750	477
4	500	477
5	1500	238
6	334	358
7	1000	358
8	250	477
9	1000	238

The wear test was performed on a computerized machine using a pin-on-disc setup. The counter disc material used in this experiment was EN 31 with a hardness of 58-60 HRC and a track diameter ranging from 20 to 140 mm. In this study, a track diameter of 80 mm (r = 40 mm) was used. This information has been included in

the manuscript as requested. The coefficient of friction (COF) and wear loss were measured using a linear variable differential transducer (LVDT). The setup for each experiment, including load, disc speed (RPM), and the required time to cover the sliding distance of tracking, was entered into the software. The required time and disc speed were calculated using Equations (4) & (5), and the calculated values for each experiment are shown in Table 5. At the end of each test, the software generated graphs and an Excel file containing the COF and wear loss recorded every second of the test as shown in Fig. 3 & 4.

$$N = \frac{V \times 30}{\pi \times r} \quad (4)$$

$$t = \frac{SD}{V} \quad (5)$$

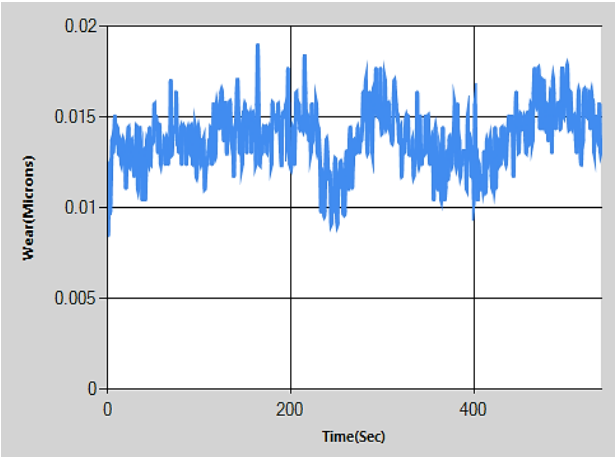

Fig. 3. Wear loss for Exp.No1 as function to time.

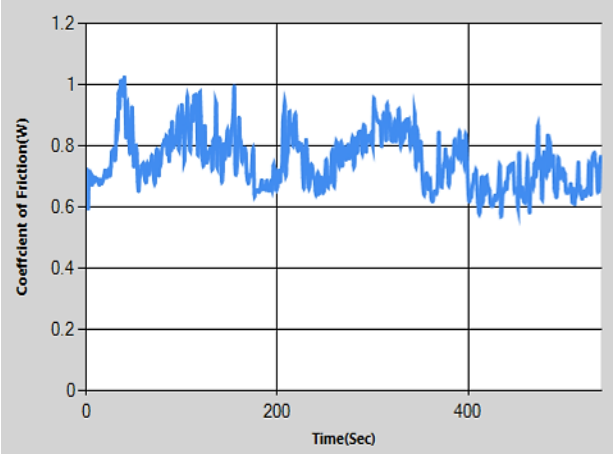

Fig. 4. COF for Exp.No1 as function to time.

In this study, the average COF was taken, and the total wear loss was considered. Table 6 shows the results of the final COF and wear loss for experiment number 1.

Where N is the disc speed (rpm), V is the sliding speed (m/s), r is the radius of the pin tracking on the disc (m) (0.04 m), SD is the sliding distance (m), and t is the required time to cover the sliding distance of tracking. The diagram illustrating the work strategy can be seen in Fig. 5.

Table 6. The wear loss and COF for the Exp. No 1.

Time (s)	Wear (Microns)	COF	Wear loss (Microns) =Sum of the wear	Avg. of COF
1	0.00849	0.7234	6.87509	0.7580
2	0.01242	0.5952		
3	0.0098	0.7094		
4	0.01176	0.7074		
5	0.01372	0.7074		
6	0.01307	0.6733		
7	0.01372	0.6974		
8	0.01503	0.6933		
9	0.01372	0.6833		
10	0.01372	0.6954		
Continue	Continue	Continue		
500	0.01699	0.6874		

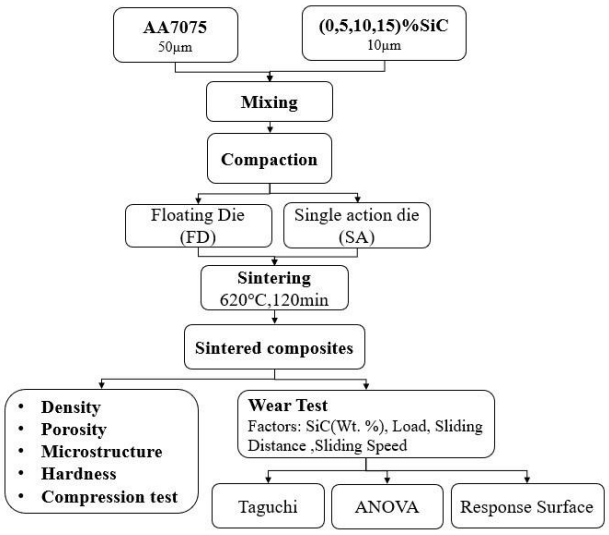

Fig. 5. Methodology.

3. RESULTS AND DISCUSSIONS

3.1 Microstructure

The dispersion of reinforcing particles in the matrix material was examined using microstructural analysis because it is a crucial factor affecting the tribological and mechanical properties of the AA7075/SiC composites. Photographs of the optical microstructure of composites reinforced with 0%, 5%, 10%, and 15% SiC by weight are shown in Fig. 6.

As demonstrated in Fig. 6(a-b), the microstructural pictures of the samples show that the A-SA composite, which was manufactured using a single-action die, had a greater pore count than the A-FD composites, which were fabricated using a floating die.

Furthermore, Fig. 6c shows a homogeneous distribution of SiC particles in the AA7075 matrix, and agglomeration of SiC particles is not found in A5S-FD composites when the SiC content is increased by 5%. Nevertheless, as Fig. 6d and 6e demonstrate, agglomeration is seen in the A10S-FD and A15S-FD composites with 10% and 15% of SiC, respectively.

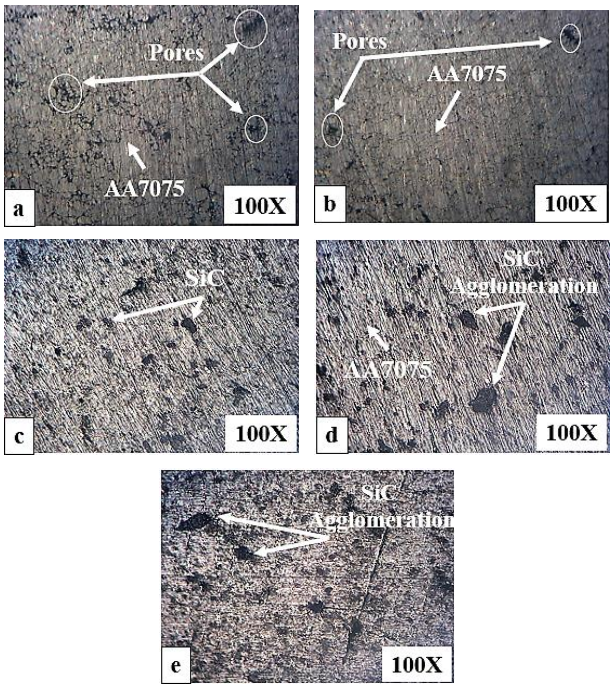

Fig. 6. Microstructure of the sintered composites :(a) A-SA, (b)A-FD, (c)A5S-FD, (d)A10S-FD, (e)A15S-FD.

3.2 Density & porosity

The variation between the theoretical and measured densities of the AA7075/SiC composites is shown in Fig. 7a. The measured and theoretical density values follow a similar trend and show close agreement. The higher density of SiC particles (3.21 g/cc) is the reason for the increasing density of the composites [35].

As seen in Fig. 7b, the porosity of the A-SA composite was higher (17%) than that of the A-FD composite (13%). Porosity increased similarly as the content of SiC increased from 5% to 15% in the composite. The composites containing SiC particles showed greater porosity than the unreinforced ones. Many factors influencing composite porosity are compaction pressure, aspect ratio of the sample, and sintering temperature.

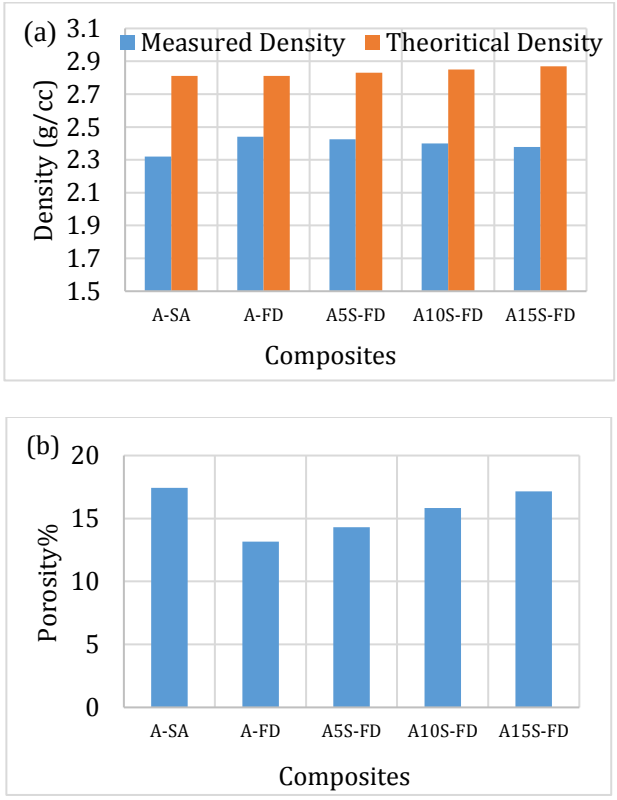

Fig. 7. (a) Theoretical and measured density (b) porosity.

The porosity of composites fabricated using the powder metallurgy route was significantly affected by the aspect ratio of the sample. In this study, we used an aspect ratio (H/D) of 25/13 = 1.99, and this sample was used for evaluating the porosity. As the aspect ratio in our study is high, it is expected that the porosity level in the sample would be high.

Previous studies confirm this. For instance, D. Dong et al. studied the effect of different aspect ratios (0.4, 0.6, 0.8, 1, 1.2, 1.4, 1.6) on the relative density of copper powder samples. They found that as the aspect ratio increased from 0.4 to 1.6, the relative density decreased from 94% to 82%, which corresponds to an increase in porosity from 6% to 18% [36]. Similarly, S. Shruthi et al. studied the effect of different aspect ratios (0.5, 1) on the final porosity of copper samples. They found that as the aspect ratio increased from 0.5 to 1, the porosity level increased from 1.29% to 5.12% [37].

3.3 Hardness

The hardness values of the AA7075/SiC composites are depicted in Fig. 8. It is clear that the A5S-FD composite, which has 5% SiC, has much higher hardness values than the unreinforced composites (A-SA and A-FD). This is because the ductile material became more brittle by adding hard ceramic reinforcement (SiC), which increases the composite's hardness at the expense of ductility [38]. On the other hand, the A10S-FD and A15S-FD composites lose hardness when the SiC fraction exceeds 5%.

The high concentration of SiC is the cause of the hardness decrease. The sample with 5 weight percent SiC was harder than the others because the reinforcement was evenly distributed throughout the matrix, allowing for strong bonding. Conversely, the 10 wt.% and 15 wt.% SiC composites displayed lower hardness due to porosity and SiC agglomerations, as depicted in the microstructure image in Fig. 8.

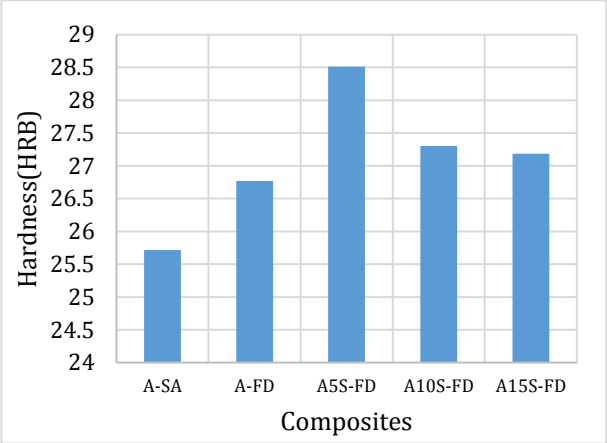

Fig. 8. Hardness.

3.4 Compression strength

The compression test was employed to assess the compressive strength of the samples. Fig. 9 shows the relationship between displacement and compressive strength for AA7075/SiC composites. Compared to the other composites, the AA5S-FD composite, which has 5% SiC, exhibits greater compressive strength. This increased strength is due to the uniform dispersion of SiC particles within the matrix and strong interfacial bonding. The lower compressive strength observed in most composites is primarily caused by the presence of pores and SiC agglomerations.

Fig. 10 shows the failure modes of the AA7075/SiC specimens. The failure mechanism of the unreinforced composite made using a single-action die (A-SA) is clearly shown in the picture. It starts at the bottom of the sample (indicated by the red circle and arrow) and moves along the sample. In contrast, when the same composite is made using a floating die (A-FD), the failure starts in the middle of the composite. This can be explained by the fact that the floating die produces a more homogeneous compact along the compaction axis with respect to its mechanical and physical properties [24]. The composite materials A-SA, A-FD, A5S-FD, A10S-FD, and A15S-FD have documented compressive strengths of 174.5 MPa, 329 MPa, 348.2 MPa, 294.3 MPa, and 207.7 MPa, respectively. This suggests that the compressive strength of the unreinforced composite (A-FD) increased by 88.9% when the floating die (FD) was used for compaction instead of the single-action die (A-SA).

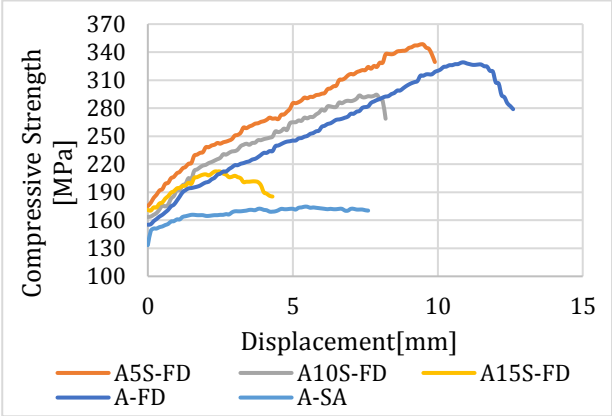

Fig. 9. Displacement vs compressive strength.

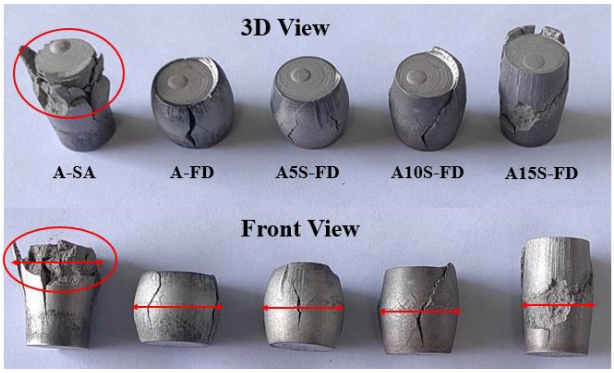

Fig. 10. The failure models after compression test.

Compared to earlier studies, some researchers, such as P. Bharathi et al., have investigated AA7075-based matrix composites and examined the effects of silicon and boron carbides on the mechanical characteristics of these composites. The hybrid AA7075/2%SiC/2%B4C composite

and AA7075/3%SiC composite had the highest compressive strengths, at 190 MPa and 240 MPa, respectively [39]. G.A. Kumar et al. studied the effects of sintering temperature and weight percentage of B4C (0, 5, 10, 15) on the mechanical properties of AA7075. When the AA7075/15%B4C composite was sintered for two hours at 600°C, the highest compressive strength of 290 MPa was attained [40].

G. Manohar et al. conducted research on hybrid composites of China clay/B4C/AA7075. They found that the composite with 6% B4C, 7% China Clay, and AA7075 had the highest compressive strength, which was 228 MPa [29].

Compared to previous studies, it was found that the AA7075 alloy reinforced with 5% SiC shows a notable increase in compressive strength of approximately 20.1% (348.2 MPa) and a weight reduction of 13.7% (2.425 g/cc). These advancements in strength and weight reduction meet critical criteria for automotive, defense, and aerospace applications.

3.5 Impact of tribological factors on the COF and wear loss of AA7075/SiC samples

The ANOVA approach was used to calculate the contribution proportion of affecting factors. Using Equation (6), the 'smaller the better' S/N ratio characteristic was applied to compute wear loss and COF [41].

Table 7. Statistical findings for the COF and wear loss of AA7075/SiC samples.

Exp. No	Results		S/N ratio	
	Wear (Microns)	COF	Wear	COF
1	6.87509	0.7580	-13.788	2.4066
2	9.32082	0.3677	-16.385	8.6901
3	18.5789	0.4939	-22.373	6.1272
4	17.1091	0.1680	-21.655	15.4938
5	35.0859	0.2367	-27.893	12.5160
6	6.06396	0.6670	-12.697	3.5175
7	26.1482	0.6743	-25.341	3.4229
8	5.88555	0.6484	-12.438	3.7631
9	18.3742	0.9002	-22.284	0.9132

Table 7 shows the statistical results for the COF and wear loss of AA7075/SiC samples. Taguchi analysis and ANOVA findings were obtained using the Minitab software.

$$S/N = -10 * \log * (\frac{1}{n}) \sum_{i=1}^{n} (\frac{1}{y^2}) \quad (6)$$

n: number of findings, y_i : measured value for the finding (i).

Wear loss is influenced by process parameters, as shown in Fig. 11. Wear loss was observed to increase with the amount of SiC. This behavior can be explained by the agglomeration of SiC particles and the increasing porosity of the composite, which result in an unstable interfacial bond between SiC and the matrix. This instability increases wear loss, thereby reducing wear resistance and load capacity [42]. In the same way, wear loss decreases as load increases. Conversely, wear loss increases with increasing sliding distance and speed. This can be explained by the fact that as the load is increased from 5 to 15 N, the actual surface area of contact between the disc and the sample pin rises at higher loads. A larger number of particles can interact with the interface region and spread the stress due to the large contact surface area, which may lead to minimal wear or a stabilization case [43, 44].

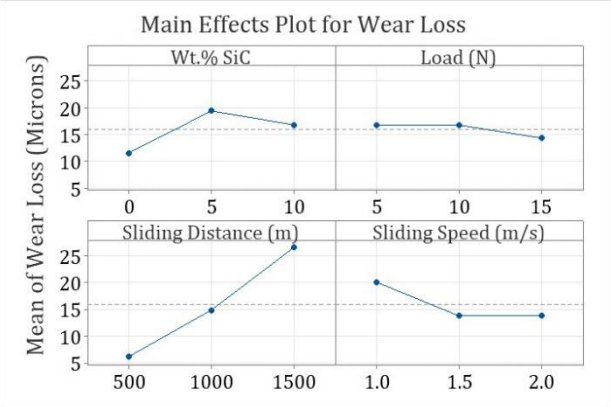

Fig. 11. Impact of process factors on the wear loss.

Fig. 12 illustrates how process factors affect COF. It was found that the COF of AA7075/SiC samples initially decreases with an increase in SiC reinforcement up to 5%, after which it rises. Similarly, increasing the load results in a lower COF, while rising sliding distance and speed lead to higher COF. This phenomenon occurs because the lower temperature prevents oxide formation between the sliding surfaces, promoting abrasion and adhesion, which increases the COF [45]. Different factors influence COF, including, the strength of the matrix-reinforcement interfacial bond, the mechanical characteristics of the matrix material, the hardness and chemical stability of the reinforcement particles, and tribological parameters [46].

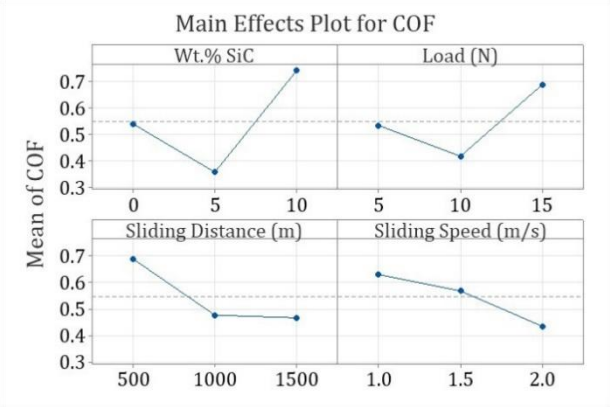

Fig. 12. Impact of process factors on the COF.

3.6 Identifying optimal parameters to minimize COF and wear loss in AA7075/SiC

It is possible to identify the control parameter that has the greatest influence on wear loss and COF by examining the S/N ratio data shown in Tables 8 and 9. The ideal parameters for wear loss and COF for the controllable variables can be determined by analyzing these ratios and examining Fig. 13 & 14.

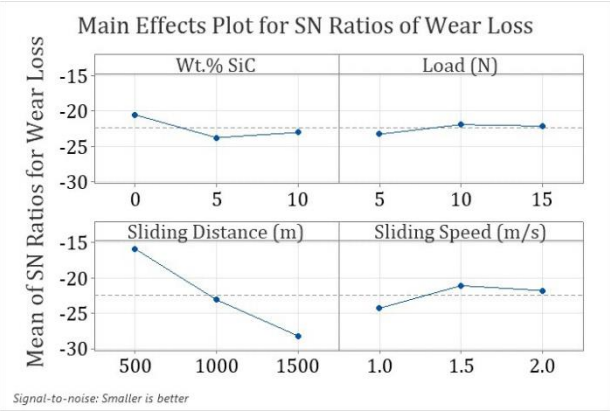

Fig. 13. Mean S/N ratio of wear.

Table 8 makes it evident that the sliding distance and weight percentage of Wt. SiC have the greatest impact on wear loss. On the other hand, Table 9 shows that the COF is most influenced by the Wt.% SiC and the sliding distance, respectively.

A greater S/N ratio denotes the least amount of variation between the intended and measured outputs, indicating the ideal parameters for lowering COF and wear loss.

Fig. 13 shows that reduced wear loss is achieved with a combination of 0% weight of SiC, 500 m sliding distance, 15 N load, and 1.5 m/s sliding speed. Likewise, examining Fig. 14, it is evident that using a 5% SiC weight, a 1000 m sliding distance, a 10 N load, and a sliding speed of 2 m/s results in a reduced COF.

However, for high strength (348.2 MPa) and low wear (6.06 Micron) in the composite, the ideal parameters are 5% of SiC, 500 m, 1.5 m/s, and 15 N.

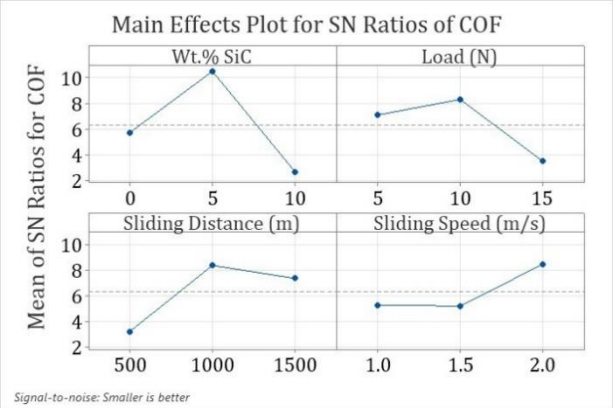

Fig. 14. Mean S/N ratio of COF.

Table 8. Response table for wear.

	Factors	Level I	Level II	Level III	Delta	Rank
W	Wt.% SiC	11.59	19.42	16.80	7.82	2
L	Load (N)	16.71	16.76	14.33	2.42	4
SD	Sliding Distance (m)	6.27	14.93	26.60	20.32	1
SS	Sliding Speed (m/s)	20.11	13.84	13.85	6.26	3

Table 9. Response table for COF.

	Factors	Level I	Level II	Level III	Delta	Rank
W	Wt.% SiC	5.741	10.509	2.700	7.809	1
L	Load (N)	7.108	8.323	3.519	4.804	3
SD	Sliding Distance (m)	3.229	8.366	7.355	5.137	2
SS	Sliding Speed (m/s)	5.279	5.210	8.461	3.251	4

3.7 ANOVA

ANOVA analysis shows the factors that have a substantial impact on the final attributes of the composites. The wear loss and coefficient of friction (COF) of ANOVA analysis are presented in

Tables 10 and 11, respectively. Table 10 indicates that sliding distance, weight percentage of SiC, sliding speed, and load have the greatest effects on wear loss, contributing 77.13%, 11.77%, 9.68%, and 1.42%, respectively.

Table 10. ANOVA for wear.

The source	D.F	S. S	M.S	Contribution %
Wt.% SiC	2	95.282	47.641	11.77
Load (N)	2	11.509	5.755	1.42
Sliding Distance (m)	2	624.460	312.230	77.13
Sliding Speed (m/s)	2	78.392	39.196	9.68
Residual Error	0	0	0	0
Total	8	809.643		100.00

Table 11. ANOVA for COF.

The source	D.F	S. S	M.S	Contribution %
Wt.% SiC	2	92.969	46.4844	47.54
Load (N)	2	37.431	18.7153	19.14
Sliding Distance (m)	2	44.432	22.2162	22.72
Sliding Speed (m/s)	2	20.705	10.3525	10.59
Residual Error	0	0	0	0
Total	8	195.537		100.00

Likewise, Wt.% SiC has the greatest impact on COF, which is then predominantly controlled by sliding distance, load, and sliding speed. Table 11 shows the percentage contributions of all of these factors to COF, which are 47.54.2%, 22.72%, 19.14%, and 10.59 %, respectively.

3.8 Modeling

In this study, the response surface method was utilized with the Minitab software tool to construct predictive mathematical Equations (7) & (8) for wear and COF respectively. Equations (7) & (8) represent the relationships with silicon carbide proportion (W), sliding distance (SD), load (L), and sliding speed (SS). These equations are as follows:

- For wear: Eqn. (7)

$$Wear\ (Microns) = 30.07 + 2.610 * W + 0.7542 * L + 0.008290 * SD - 43.94 * SS - 0.2089 * W^2 - 0.04957 * L^2 + 0.000006 * SD^2 + 12.56 * SS^2 \quad (7)$$

- For the COF: Eqn. (8)

$$COF = 1.585 - 0.09316 * W - 0.1387 * L - 0.001032 * SD + 0.2307 * SS + 0.01133 * W^2 + 0.007705 * L^2 + 0.00000040397 * SD^2 - 0.1419 * SS^2 \quad (8)$$

To determine the ideal values, the values corresponding to the optimal levels of process parameters were entered into Equation (7) to predict low wear. For example, the best wear value is found to be 4.39 microns at SiC weight % = 0, sliding distance = 500 m, load = 15 N, and sliding speed = 1.5 m/s. Likewise, Equation (8) was used to calculate the ideal coefficient of friction (COF), yielding a value of 0.0522 for the following ideal parameters: load = 10 N, sliding speed = 2 m/s, and SiC weight percentage = 5.

3.9 Experimental validation

At ideal parameters, the prediction equations for COF and wear loss were validated experimentally. Table 12 presents a thorough comparison of the experimental and regression equation results.

Table 12. A comparative analysis of regression equation results and experimental findings.

Results	Wear (Microns)	COF
Regression equations results	4.39	0.0522
Experimental results	4.84	0.0621
Error	9.3%	15.9%

Furthermore, the experimental results and those predicted by the equations for wear loss and COF differ by less than 10% and 15.9%, respectively. These findings imply that the regression equations yield appropriate results and can be relied upon to compute the response property values for new parameter sets.

Minitab software was utilized to create surface and contour plots to examine the relationship between two process factors and the outcome property. Surface and contour graphs in Fig. 15 show the relationship between wear and several parameters. The findings presented in Fig. 15 (a-b) suggest that reduced wear can be attributed to both load levels (15 N) and silicon carbide levels (0%). Furthermore, the contour plots and surface plots for wear related to sliding speed and sliding distance are presented in Fig. 15 (c-d), which demonstrate that lower sliding distance and speed (500 m, 1.5 m/s) are associated with less wear.

The relationship between process parameters and the COF is shown in Fig. 16 using contour and surface plots. Observations from Fig. 16 (a-b) indicate that a load of 10 N and 5% silicon carbide both contribute to a decreased coefficient of friction. Furthermore, Fig. 16 (c-d) presents contour and surface plots for COF with respect to sliding distance and speed, demonstrating that the sliding speed and distance of 2 m/s and 1000 m are associated with reduced COF.

These results agree with the ideal process parameters for wear loss and COF as established by the Taguchi method.

In contrast to prior research, certain scholars, including K.V. Subbaiah et al., studied the wear behavior of hybrid AA6351/5%Sic/(3,6,9%) ZrO_2 composites under various parameters including sliding speed (0.5,0.84,1.34 m/s), reinforcements percentage of ZrO_2(3,6,9%), and load (10,20,30 N).they found that minimum wear loss of 174.57 microns at parameters of 9% ZrO_2,20 N, and 0.5 sliding speed [47]. Ravindra et al., have studied the tribological characteristics of Al7049/B_4C composites fabricated via stir casting. They found a minimum wear loss of approximately 200 microns under a load of 20 N and a speed of 200 RPM [48].

M.S. Surya et al., studied the impact of silicon carbide weight percentage on the mechanical and wear properties of AA7075 using powder metallurgy. They studied various tribological factors, including sliding distance (500, 1000, 1500 m), SiC weight percentage (5, 10, 15%), and load (10, 15, 20 N), on wear behavior. They found a minimum wear loss of 69 microns (1.951mm^3**,** based on the sample diameter of 6 mm and the volume equation $V = \pi r^2 \times h$) [49].

In another research, they investigated the effect of Wt.% SiC (0,3,7,10%) and loads (10,15,20 N) on wear characteristics. They found that the maximum wear loss was 383 microns (19.26 mm^3) and the minimum wear loss was 36.26 microns (1.822 mm^3) for composite containing 10 % SiC [50].

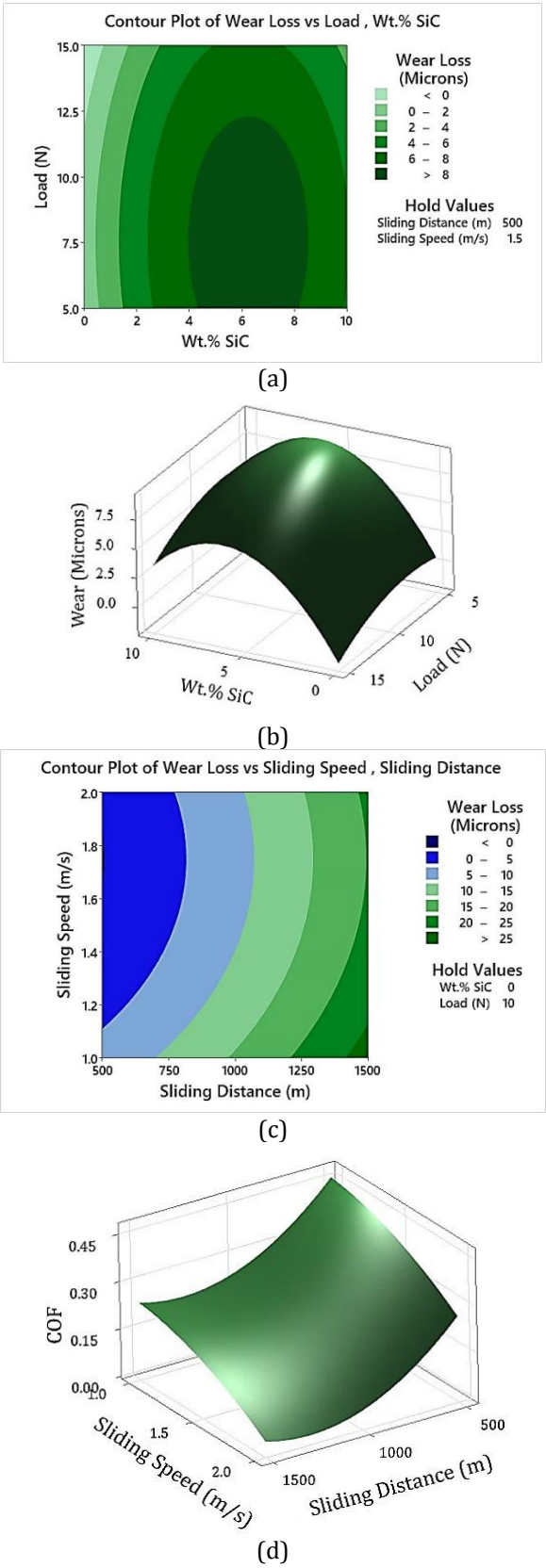

Fig. 15. Contour plots and surface plots for wear (a) Wear contour plot versus load and SiC% (b) Wear surface plot versus load and SiC % (c) Wear contour plot versus sliding speed and sliding distance (d) Wear surface plot versus sliding speed and sliding distance.

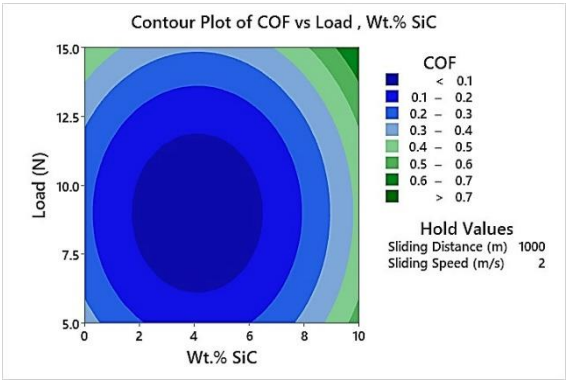

(a)

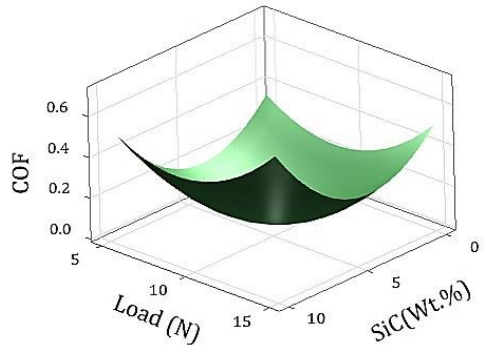

(b)

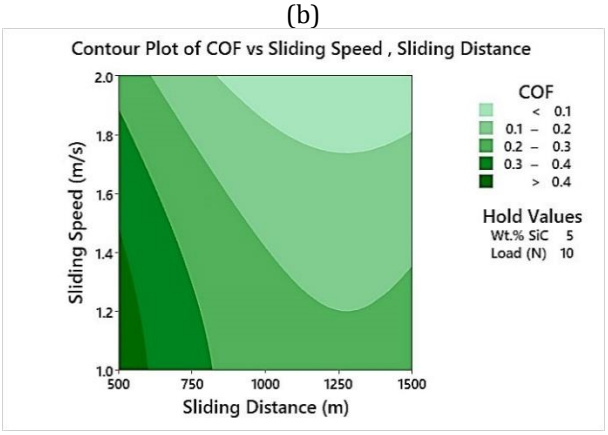

(c)

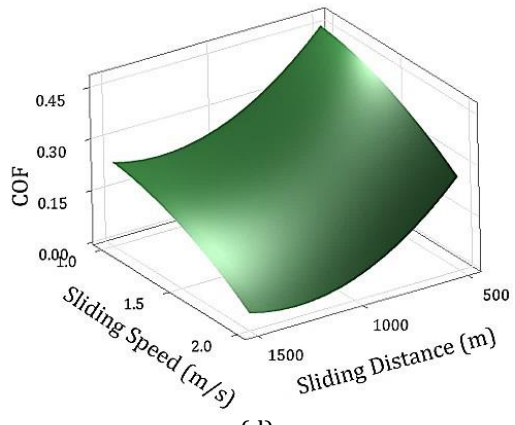

(d)

Fig. 16. Contour plots and surface plots for COF (a) COF contour plot versus load and SiC % (b) COF plot versus load and SiC % (c) COF contour plot versus sliding speed and sliding distance (d) COF surface plot versus sliding speed and sliding distance.

The minimum wear loss observed in the previous studies was 36.26 microns, whereas in our study it was 6.06 microns under parameters of 500 m,1.5 m/s, and 15 N for AA7075/5%SiC composite which exhibited the highest strength (348.2 MPa). In comparison with prior research, our study achieved a significant improvement of 83.28% (6.06 microns).

4. CONCLUSIONS

The innovative floating die was used successfully for preparing (0, 5, 10, 15) % SiC/AA7075 composites using the powder metallurgy route. The physical, mechanical, and microstructural properties of these composites were studied. Moreover, the effect of tribological parameters including load (5,10,15 N), sliding speed (1,1.5,2 m/s), wt.% SiC (0,5,10 %), and sliding distance (500,1000,1500 m) on the wear performance of AA7075/SiC were studied and analyzed using Taguchi, ANOVA, and response surface methods. The main findings from this study are:

- AA7075/5% SiC composite exhibited a uniform distribution of SiC particles in the AA7075 matrix; however, agglomeration was observed at 10% and 15% of SiC.
- The density of the composites increased with the increase in wt.% SiC because the theoretical density of SiC is higher than that of AA7075.
- The composites fabricated using the floating die showed a more homogeneous failure model under compression tests compared with the single-action die.
- The ideal parameters for achieving the lowest wear loss are a 0% SiC, a sliding distance of 500 m, a sliding speed of 1.5 m/s, and a load of 15 N. Conversely, for minimizing the COF, the ideal parameters are a sliding distance of 1000 m, 5% SiC, a sliding speed of 2 m/s, and a load of 10 N.
- The variance between the regression equation values and experimental findings was 15.9% for COF and 9.3% for wear loss. This shows a good agreement between experimental results and predictive regression equations.
- Wear loss was significantly influenced by sliding distance (77.13%), followed by Wt.% SiC (11.77%), sliding speed (9.68%), and load

(1.42%). Meanwhile, COF was significantly influenced by the weight percentage of SiC (47.54%), followed by sliding distance (22.72%), load (19.14%), and sliding speed (10.59%), respectively.

- In comparison to earlier research, the findings demonstrate a significant enhancement in compressive strength showing an increase of approximately 20.1% (348.2 MPa), alongside a reduction in weight of 14.7% (2.425 g/cc), and an 83.28% (6.06 microns) reduction in wear loss for the AA7075 alloy reinforced with 5% SiC under tribological parameters of 15 N,500 m, and 1.5 m/s. These improvements in strength, weight reduction, and wear loss are pivotal considerations for applications in the aerospace, defense, and automotive industries.

REFERENCES

[1] M.S. Surya, G. Prasanth, "Tribological behavior of aluminum silicon carbide functionally graded material," *Tribology in Industry*, vol. 40, no. 2, pp. 247-253, Jun. 2018, doi: 10.24874/ti.2018. 40.02.08.

[2] W.S. Miller, L. Zhuang, J. Bottema, A.J. Wittebrood, P.De. Smet, A. Haszler, A. Vieregge, "Recent development in aluminium alloys for the automotive industry," *Materials Science and Engineering: A*, vol. 280, no. 1, pp. 37–49, Mar. 2000, doi: 10.1016/S0921-5093(99)00653-X.

[3] P.L. Kumar, A. Lombardi, G. Byczynski, S.N Murty, B.S. Murty, L. Bichler, "Recent advances in Aluminium matrix composites reinforced with graphene-based nanomaterial: A critical review," *Progress in Materials Science*, vol. 128, p. 100948, Jul. 2022, doi: 10.1016/j.pmatsci.2022. 100948.

[4] M.A. Alam, H.B. Ya, M. Azeem, M. Mustapha, M. Yusuf, F. Masood, R.V. Marode, S.M. Sapuan, A.H. Ansari, "Advancements in aluminium matrix composites reinforced with carbides and graphene: A comprehensive review," *Nanotechnology Reviews,* vol. 12, no. 1, p. 20230111, Nov. 2023, doi: 10.1515/ntrev-2023-0111.

[5] M.M. Boopathi , K.P. Arulshri and N. Iyandurai, "Evaluation of mechanical properties of Aluminium alloy 2024 reinforced with silicon carbide and fly ash hybrid metal matrix composites," *American journal of applied sciences*, vol. 10, no. 3, pp. 219-229, Mar. 2013, doi: 10.3844/ajassp.2013.219.229.

[6] G.V. Kumar, C.P. Rao, N. Selvaraj, "Mechanical and tribological behaviour of particulate reinforced aluminium metal matrix composites–a review," *Journal of minerals and materials characterization and engineering*, vol. 10, no. 1, pp. 59-91, Jan. 2011, doi: 10.4236/JMMCE. 2011.101005.

[7] A.J. Dolata, M. Dyzia, J. Wieczorek, "Tribological properties of single (AlSi7/SiCp, AlSi7/GCsf) and hybrid (AlSi7/SiCp+ GCsf) composite layers formed in sleeves via centrifugal casting," *Materials*, vol. 12, no. 17, p. 2803, Aug. 2019, doi: 10.3390/ma12172803.

[8] N. Radhika, J. Sasikumar, J. Arulmozhivarman, "Tribo-mechanical behaviour of Ti-based particulate reinforced as-cast and heat treated A359 composites," *Silicon*, vol. 12, no. 11, pp. 2769-2782, Nov. 2020, doi: 10.1007/s12633-019-00370-8.

[9] M.S. Surya, G. Prasanthi, "Manufacturing, microstructural and mechanical characterization of powder metallurgy processed Al7075/SiC metal matrix composite," *Materials Today: Proceedings*, vol. 39, pp. 1175-1179, Jan. 2021, doi: 10.1016/j.matpr.2020.03.3156.

[10] M.S. Surya, G. Prasanthi, "Manufacturing and mechanical behavior of (Al/SiC) functionally graded material using powder metallurgy technique," *Int J Innovative Technol Explor Eng*, vol. 8, no. 9, pp. 1835–18397, Jul. 2019, doi: 10.35940/ijitee.i8215.078919.

[11] G.V. Kumar, C.S.P. Rao, N. Selvaraj, M.S. Bhagyashekar, "Studies on Al6061-SiC and Al7075-Al 2 O 3 metal matrix composites," *Journal of Minerals and Materials Characterization and Engineering*, vol. 9, no. 1, pp. 43-55, Jan. 2010, doi: 10.4236/jmmce. 2010.91004.

[12] C.R. Mahesha, M.M. Sree Jayan, S. Kulkarni, A. Sharma, E.A. Al-Ammar, S.M.A.K. Mohammed, R. Subbiah, A. Alemayehu, "Tribological Behavior of AA7075 Reinforced with Ag and ZrO_2 Composites," *Advances in Materials Science and Engineering*, vol. 2022, no. 1, pp. 7105770, Sep. 2022, doi: 10.1155/2022/7105770.

[13] H.M. Xia, L. Zhang, Y.C. Zhu, N. Li, Y.Q. Sun, J.D. Zhang, and H.Z. Ma, "Mechanical properties of graphene nanoplatelets reinforced 7075 aluminum alloy composite fabricated by spark plasma sintering," *International Journal of Minerals, Metallurgy and Materials*, vol. 27, pp. 1295-1300, Sep. 2020, doi: 10.1007/s12613-020-2009-0.

[14] A. Sridhar, and K.P. Lakshmi, "Evaluation of mechanical and wear properties of aluminum 7075 alloy hybrid nanocomposites with the additions of SiC/Graphite," *Materials Today: Proceedings*, vol. 44, pp. 2653-2657, Jan. 2021, doi: 10.1016/j.matpr.2020.12.675.

[15] A.R. Rajendran, A.P. Dhanaraj, J.K. Sadhasivam, A. Mani, and M.A. Qureshi, "Optimization of Process Parameters of Aluminium 7075/TiCnp MMC Fabricated Using Powder Metallurgy Route," *Engineering Proceedings*, vol. 61, no. 1, p. 49, Feb. 2024, doi: 10.3390/engproc2024061049.

[16] F. Aydin, "The investigation of the effect of particle size on wear performance of AA7075/Al2O3 composites using statistical analysis and different machine learning methods," *Advanced Powder Technology*, vol. 32, no. 2, pp. 445-463, Feb. 2021, doi: 10.1016/j.apt.2020.12.024.

[17] A. Mazahery, M.O. Shabani, "Study on microstructure and abrasive wear behavior of sintered Al matrix composites," *Ceramics International*, vol. 38, no. 5, pp. 4263-4269, Jul. 2012, doi: 10.1016/j.ceramint.2012.02.008.

[18] A. Vencl, A. Rac, I. Bobic, "Tribological behaviour of Al-based MMCs and their application in automotive industry," *Tribology in industry*, vol. 26, no. (3-4), pp. 31-38, Dec. 2004.

[19] M.S. Surya, T.V. Nilesh, "Synthesis and mechanical behaviour of (Al/SiC) functionally graded material using powder metallurgy technique," *Materials Today: Proceedings*, vol. 18, pp. 3501-3506, Jan. 2019, doi: 10.1016/j.matpr.2019.07.278.

[20] A. Al Njjar, K. Mazloum, A. Sata, "Simulation of the die and punch behaviour during the compaction process of alumina-based matrix composite using finite element analysis," *Recent Patents on Mechanical Engineering*, vol. 17, no. 5, pp. 365–379, 2024, doi: 10.2174/0122127976307663240326153651.

[21] P.C. Angelo, R. Subramanian, B. Ravisankar, "Powder Metallurgy: Science, Technology and Applications," 2nd ed. PHI Learning Pvt. Ltd, 2022.

[22] S. Sattari, M. Jahani, A. Atrian, "Effect of volume fraction of reinforcement and milling time on physical and mechanical properties of Al7075–SiC composites fabricated by powder metallurgy method," *Powder Metallurgy and Metal Ceramics*, vol. 56, no. 5, pp. 283-292, Sep. 2017, doi: 10.1007/s11106-017-9896-2.

[23] A.E. Nassar, E.E. Nassar, "Properties of aluminum matrix Nano composites prepared by powder metallurgy processing," *Journal of king saud university-Engineering sciences*, vol. 29, no. 3, pp. 295-299, Jul. 2017, doi: 10.1016/j.jksues.2015.11.001.

[24] A. Al Njjar, K. Mazloum, A. Sata, "Comparison of single action die and floating die for compaction of aluminum alloy AA7075 using simulation and experimental study," *Engineering Research Express*, vol. 6, no. 1, p. 015412, Mar. 2024, doi: 10.1088/2631-8695/ad3478.

[25] R.K. Bhushan, S. Kumar, "Influence of SiC particles distribution and their weight percentage on 7075 Al alloy," *Journal of materials engineering and performance*, vol. 20, pp. 317-323, Mar. 2011, doi: 10.1007/s11665-010-9681-6.

[26] P.V. Reddy, P.R. Prasad, D.M. Krishnudu, E.V. Goud, "An investigation on mechanical and wear characteristics of Al 6063/TiC metal matrix composites using RSM," *Journal of Bio-and Tribo-corrosion*, vol. 5, no. 4, p. 90, Dec. 2019, doi: 10.1007/s40735-019-0282-0.

[27] N. Faisal, K. Kumar, "Mechanical and tribological behavior of nano scaled silicon carbide reinforced Aluminium composites," *Journal of Experimental Nanoscience*, vol. 13, no. sup1, pp. S1-S13, Feb. 2018, doi: 10.1080/17458080.2018.1431846.

[28] M.S. Surya, G. Prasanthi , S.K. Gugulothu, "Investigation of mechanical and wear behavior of Al7075/SiC composites using response surface methodology," *Silicon*, vol. 13, no. 7, pp. 2369-2379, Jul. 2021, doi: 10.1007/s12633-020-00854-y.

[29] G. Manohar, K.M. Pandey, S.R. Maity, "Effect of china clay on mechanical properties of AA7075/B4C hybrid composite fabricated by powder metallurgy techniques," *Materials Today: Proceedings*, vol. 45, pp. 6321-6326, Nov. 2021, doi: 10.1016/j.matpr.2020.10.740.

[30] N. Kumar, G. Gautam, R.K. Gautam, A. Mohan, S. Mohan, "Synthesis and characterization of TiB 2 reinforced Aluminium matrix composites: a review," *Journal of The Institution of Engineers (India): Series D*, vol. 97, pp. 233-253, Oct. 2016, doi: 10.1007/s40033-015-0091-7.

[31] V.S.S. Venkatesh, A.B. Deoghare, "Effect of boron carbide and Kaoline reinforcements on the microstructural and mechanical characteristics of Aluminium hybrid metal matrix composite fabricated through powder metallurgy technique," *Advances in Materials and Processing Technologies*, vol. 8, no. sup2, pp. 1007-1028, Sep. 2022, doi: 10.1080/2374068X.2021. 1945314.

[32] M.S. Surya, G. Prasanthi, "Effect of silicon carbide weight percentage and number of layers on microstructural and mechanical properties of Al7075/SiC functionally graded material," *Silicon*, vol. 14, no.4, pp. 1339-1348, Feb. 2022. doi: 10.1007/s12633-020-00865-9.

[33] G. Manohar, K.M. Pandey, S.R. Maity, "Effect of microwave sintering on the microstructure and mechanical properties of AA7075/B4C/ZrC hybrid nano composite fabricated by powder metallurgy techniques," *Ceramics International*, vol 47, no. 23, pp. 32610-8, Dec. 2021, doi: 10.1016/j.ceramint.2021.08.156.

[34] P. Ravindran, K. Manisekar, R. Narayanasamy, P. Narayanasamy, "Tribological behavior of powder metallurgy-processed Aluminium hybrid composites with the addition of graphite solid lubricant," *Ceramics International*, vol. 39, no. 2, pp. 1169-1182, Mar. 2013, doi: 10.1016/j.ceramint.2012.07.041.

[35] S. Sahoo, S. Samal, B. Bhoi, "Fabrication and characterization of novel Al-SiC-hBN self-lubricating hybrid composites," *Materials Today Communications*, vol. 25, p. 101402, Dec. 2020, doi: 10.1016/j.mtcomm.2020.101402.

[36] D. Dong, X. Huang, J. Cui, G. Li, H. Jiang, "Effect of aspect ratio on the compaction characteristics and micromorphology of copper powders by magnetic pulse compaction," *Advanced Powder Technology*, vol. 31, no. 10, pp. 4354-4364, Oct. 2020, doi: 10.1016/j.apt.2020.09.010.

[37] S. Shruthi, S. Venkatakrishnan, S. Raghuraman, R. Venkatraman, "Effect of Compaction Aspect Ratio on Wear Characteristics of Sinter Extruded Pure Copper Processed Through Powder Metallurgy Route," Lecture Notes in Mechanical Engineering, 2016, pp. 379-384, doi: 10.1007/978-981-10-1771-1_40.

[38] G. Manohar, K.M. Pandey, S.R. Maity, "Effect of processing parameters on mechanical properties of Al7175/Boron Carbide (B4C) composite fabricated by powder metallurgy techniques," *Advances in Science and Technology*, vol. 105, pp. 8-16, Jun. 2021, doi: 10.4028/www.scientific.net/AST.105.8.

[39] P. Bharathi, T. S. Kumar, "Effect of Silicon Carbide and Boron Carbide on Mechanical and Tribological Properties of Aluminium 7075 Composites for Automobile Applications," *Silicon*, vol. 15, no. 14, pp. 6147-6171, Sep. 2023, doi: 10.1007/s12633-023-02498-0.

[40] G.A. Kumar, J. Sateesh, T.Y. Kumar, T. Madhusudhan, "Properties of Al7075-B4C composite prepared by powder metallurgy route," *International Research Journal of Engineering and Technology*, vol. 3, no. 7. pp. 2315-2319, 2016.

[41] D. Dey, A. Biswas, "Comparative study of physical, mechanical and tribological properties of Al2024 alloy and SiC-TiB 2 composites," *Silicon*, vol. 13, pp. 1895-1906, Jun. 2021, doi: 10.1007/s12633-020-00560-9.

[42] N. Singh, I.U.H. Mir, A. Raina, A. Anand, V. Kumar, S.M. Sharma, "Synthesis and tribological investigation of Al-SiC based nano hybrid composite," *Alexandria engineering journal*, vol. 57, no. 3, pp. 1323-1330, Sep. 2018, doi: 10.1016/j.aej.2017.05.008.

[43] Y. Şahin, "Analysis of abrasive wear behavior of PTFE composite using Taguchi's technique," *Cogent Engineering*, vol. 2, no. 1, p. 1000510, Dec. 2015, doi: 10.1080/23311916.2014.1000510.

[44] C. Anand, S.P. Kumaresh, "Influence of titanium carbide on the three-body abrasive wear behaviour of glass–fabric reinforced epoxy composites," *Advances in Materials*, vol. 1, pp. 9-15, Dec. 2012, doi: 10.11648/j.am.20120101.12.

[45] J. Babu Rao, D. Venkata Rao, K. Siva Prasad, N.R.M.R. Bhargava, "Dry sliding wear behavior of fly ash particles reinforced AA 2024 composites," *Materials Science-Poland*, vol. 30, pp. 204-211, Sep. 2012, doi: 10.2478/s13536-012-0026-z.

[46] D. Dey, A. Biswas, "Comparative study of physical, mechanical and tribological properties of Al2024 alloy and SiC-TiB 2 composites," *Silicon*, vol. 13, pp. 1895-1906, Jun. 2021, doi: 10.1007/s12633-020-00560-9.

[47] K.V. Subbaiah, T.S. Naidu "Wear performance of Aluminium hybrid nanocomposites using Taguchi," *Engineering Research Express*. vol. 6, p. 025011, Jun. 2024, doi: 10.1088/2631-8695/ad4b95.

[48] Ravindra,M. Rajesh, K. D. Kumar, M. Sailender, G. P. Prasad, N. Nagaraj, P. J. Ramulu, "Effect of boron carbide particles addition on the mechanical and wear behavior of Aluminium alloy composites," *Advances in Materials Science and Engineering*, vol. 2023, pp. 1-10, Apr. 2023, doi: 10.1155/2023/2386558.

[49] M.S. Surya, S.K. Gugulothu, "Fabrication, mechanical and wear characterization of silicon carbide reinforced Aluminium 7075 metal matrix composite," *Silicon*, vol. 14, no. 5, pp. 2023-2032, Apr. 2022, doi: 10.1007/s12633-021-00992-x.

[50] M.S. Surya, G. Prasanthi, "Tribological behavior of aluminum silicon carbide functionally graded material," *Tribology in Industry*, vol. 40, no. 2, p. 247-253, Jun. 2018, doi: 10.24874/ti.2018.40.02.08.